Journal of Magnetic Resonance 197 (2009) 48–55

Contents lists available at ScienceDirect

Journal of Magnetic Resonance

journal homepage: www.elsevier.com/locate/jmr

Simulation of DNMR spectra using propagator formalism and Monte Carlo method

Zsófia Szalay, János Rohonczy *

Department of Inorganic Chemistry, Institute of Chemistry, Eötvös Loránd University, H-1518 Budapest 112. Pf: 32, Hungary

ARTICLE INFO

Article history:
Received 10 September 2008
Revised 28 November 2008
Available online 11 December 2008

Keywords:
DNMR
Dynamic NMR spectrum simulation
Monte Carlo method
Propagator
Density matrix

ABSTRACT

A new program—ProMoCS—is presented for the simulation of dynamic nuclear magnetic resonance spectra. Its algorithm is based on the Monte Carlo method as the one of the previously introduced MC-DNMR but the theory of ProMoCS is explained by using the statistical approach of propagator formalism. Our new program is suitable for the calculation of dynamic NMR spectra of spin systems up to 12 ½ spin nuclei, several conformers and any type of exchange between them. Mutual exchange of coupled spins can be simulated as well. While it keeps the main advantage of the Monte Carlo based method: calculation with significantly smaller matrices as compared with programs based on the simulation of the average density matrix, the maximum number of nuclei is increased significantly. Thus spectra of such systems can be simulated that was impossible previously.

1. Introduction

Methods for the simulation of dynamic NMR spectra are well-known for systems with chemical exchange [1–7]. The most widespread simulation programs (DNMR5 [8–11], MEXICO [12–14], WinDNMR [15–16], Bruker's TOPSPIN DNMR module [17]) are based on the calculation of transitions using the average density matrix. The most important limitation of this method is the huge computer memory requirement even for simple spin systems. In the case of a spin system with n nuclei and s conformers the dimension of the coefficient matrix is proportional to $s{\cdot}4^n$. This matrix blocks according to the coherence levels and these blocks are treated separately. The blocks with smaller sizes, the neglection of combinational transitions and the use of sparse matrix diagonalization methods [18–19] can reduce the computer memory requirement radically, but the reduced matrix still can be too big for more complicated spin systems.

Our MC-DNMR program based on the theory of Monte Carlo simulations was introduced as alternative simulation algorithm with less memory requirement previously [20]. The theory of that program was based on the extension of single spin vector model to coupled spin systems, by which the chemical exchange could be incorporated into the vector model. The memory requirement of this program is significantly smaller than that of the programs mentioned above. However, in cases of scalar coupling between the exchanging sites the simulated high temperature spectrum yields in non-realistic multiplets.

In order to correct this error the theoretical background of the Monte Carlo simulations of DNMR spectra is now presented using the propagation of individual density matrices. A new program called ProMoCS (Propagation & Monte Carlo Simulation) was written which gives correct results even in cases where MC-DNMR fails.

2. Theoretical background

The well-known method for the simulation of dynamic NMR spectra is based on the solution of Liouville–von Neumann equation [21]:

$$\frac{d\bar{\rho}}{dt} = -i[H, \bar{\rho}]. \tag{1}$$

As a first step this equation is converted into the Liouville space. This means that the average density matrix ($\bar{\rho}$, function of t time) becomes a vector ($\bar{\sigma}$) and its commutator with the Hamiltonian (H) transform to a superoperator ($\bar{L}$):

$$\frac{d\bar{\sigma}}{dt} = -i\bar{L}\bar{\sigma}. \tag{2}$$

In order to describe the relaxation and dynamic processes two additional terms are included: the Redfield-type relaxation (R) and the exchange (X) matrices, resulting in:

$$\frac{d\bar{\sigma}}{dt} = -(i\bar{L} + R + X)\bar{\sigma}. \tag{3}$$

The solution of this equation gives the evolution of the density matrix as a function of the time elapsed as:

$$\bar{\sigma}(t) = \exp(-(i\bar{L} + R + X))\bar{\sigma}_0, \tag{4}$$

* Corresponding author. Fax: +36 1 3722 909.
E-mail address: rohonczy@chem.elte.hu (J. Rohonczy).

1090-7807/$ - see front matter © 2008 Elsevier Inc. All rights reserved.
doi:10.1016/j.jmr.2008.12.002

where $\bar{\sigma}_0$ is the density matrix at the start of detection ($t = 0$). From now the relaxation is approximated with the multiplication of the time domain signal with an exponential at the end of the calculation so the matrix R can be neglected in Eq. (4). The signal (*fid*) is then calculated as the scalar product of the density matrix and the vector of the I^+ operator:

$$fid(t) = \langle I^+ | \bar{\sigma}(t) \rangle. \tag{5}$$

The *average* density matrix calculated by this method describes the average of molecular states in the whole system. This means that all sites are included in it (Fig. 1a). Spins are distinguished by their chemical environment (and chemical shift) and not by the individual nucleus they belong to. The coefficients in the density matrix represent the populations of the coherences.

For our purposes we define the *individual* density matrix (ρ or σ). This matrix describes the probabilities of the possible spin states of the nuclei in one individual molecule. From now we use the name *spin set* for these nuclei. In an exchanging system a given spin set can change its chemical environment but the nuclei remain together in it. In different chemical environments the density matrix evaluates differently (e.g. the Hamiltonian depends on the chemical environment). As molecules can convert into each other at any time, the chemical environments, Hamiltonians and propagators of spin sets are permuted randomly in time.

The *fid* of a spin set can be calculated from its own density matrix as it is shown later. The sum of the *fid*s of a few hundreds or thousands of randomly selected spin sets gives the overall *fid* which is a good approximation of the macroscopic signal (Monte Carlo method).

In order to construct the algorithm of the simulation the followings should be given: the method for the determination of the lifetimes of the conformers and the mathematical forms of the operators of precession, detection and exchange.

The time of an exchange (to be called exchange points and noted as t_r) is determined statistically based on the rate coefficients of the exchanges. The lengths of intervals between two exchange points (time slices) have exponential distribution with the average lifetime (τ_i) of the molecule as its parameter [20]:

$$t_{r+1} - t_r = -\tau_i \ln(rnd) = -\left(\sum_j k_{ij}\right)^{-1} \ln(rnd), \tag{6}$$

where *rnd* is a random number and k_{ij} is the rate coefficient of the exchange from molecule i to j.

During an exchange, which is assumed to happen in negligible time (instant jump approximation), the spin set remains unaltered, only the chemical environment and its parameters like chemical shift and coupling constants of the corresponding nucleus alter. This affects only the precession operator but not the density matrix (Fig. 1b). As a consequence the precession operator of the r-th time slice has to be replaced by a new one according to the new state in time slice $r + 1$ at the beginning of the $(r + 1)$th time slice (e.g. replace P^{AB} with P^{CD} at t_1 for $r = 1$ on Fig. 1b). After the exchange the simulation for time slice $r + 1$ is continued using $\sigma^{(r)}$ (the density matrix at t_r).

The *fid* of the r-th time slice for one molecule is calculated at the detection points that fall into the corresponding interval. If the rates of exchanges are so fast, that there are more than one exchange points between two sampling points, there must be time slices without sampling point. In the case of such 'dummy' slices only the density matrix is propagated to the end of this time slice. The *fid* of the spin set (scan) is the union of the *fid*s of the time slices and the spectrum of the whole system is calculated as the Fourier transform of the sum of the scans. This method is described in detail in Ref. [20].

As the exchange is handled as a propagating effect of the density matrix, the whole exchanging spin system (including the spins of all conformers) can be simulated by calculating with only one static (only J-coupled) spin set. Therefore the basis set used for the simulation is made of the basis functions of one spin set. The size of basis set is $\sim 2^n$ where n is the number of nuclei in the spin set. In fact the Hamiltonian, the density matrix and the precession operator blocks according to the coherence levels and the size of the largest block is only $\binom{n}{n/2}$. This size still means an exponentially scaling memory requirement but is significantly smaller than the memory needed for the conventional calculations [8–17] using density matrix blocks. The RAM requirement of the program is independent of the number of exchanging sites.

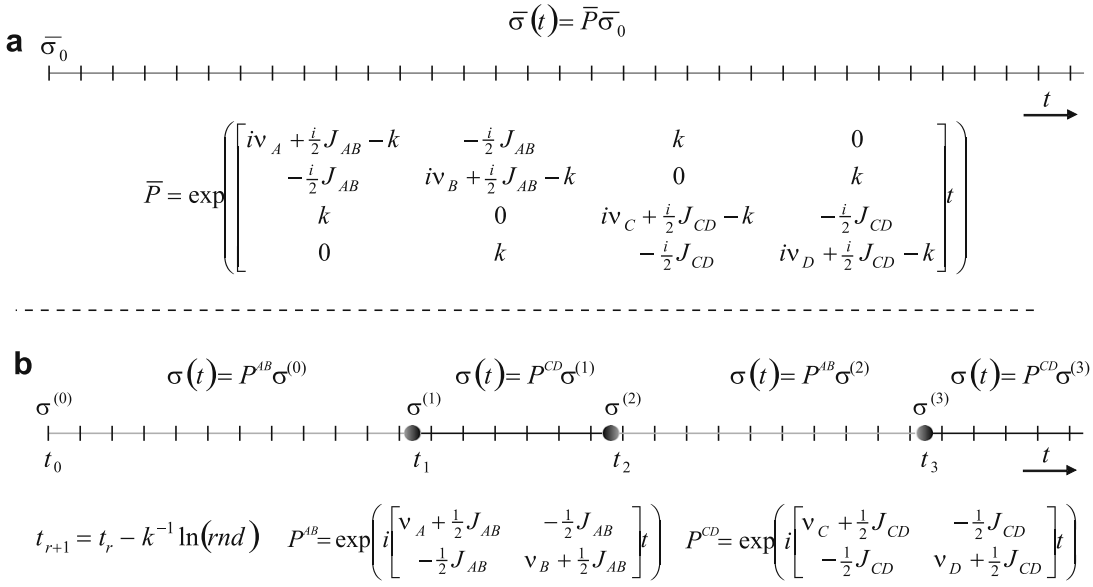

Fig. 1. Propagation of the (a) average (b) individual density matrix. Ticks show the points of detection (where *fid* points are calculated) and dots show the points of exchange. As an example, the propagators ($\bar{P}$ and P^{AB}, P^{CD}) of an exchanging AB ↔ CD spin system are shown for both calculations.

3. Mathematical formalism

Theoretical calculations are performed in the subspace of the Liouville space expanded by the one-quantum coherences of the spin set. In this space φ_e denotes the e-th basis transition (e is in the range $1\ldots2^{2n}$). The eigenfunctions of the L matrix (where $L\sigma = [H, \rho]$) of the spin system are noted by ψ_p and ω_p denotes the eigenvalue of the Hamiltonian with ψ_p.

The eigenfunctions can be written as the linear combination of basis functions:

$$\psi_p = \sum_e c_{ep}\varphi_e. \tag{7}$$

It comes from Eq. (7) that the c_{ep} coefficients can be given as the scalar product of a basis and an eigenfunction (the c_{ep} coefficients are real; therefore the scalar product is symmetrical):

$$c_{ep} = \langle\varphi_e|\psi_p\rangle = \langle\psi_p|\varphi_e\rangle. \tag{8}$$

The global time t denotes the time elapsed since the start of detection ($t = 0$ is the start of detection after the 90° pulse). The points of exchange are denoted as t_r, and Δt is the time elapsed since the last exchange ($\Delta t = t - t_r$). The length of time slice r is denoted as $\Delta t_r = t_r - t_{r-1}$. The density matrix is $\sigma(t)$ at point t and $\sigma^{(r)}$ is the short form for $\sigma(t_r)$.

3.1. Precession (propagation)

The operator of precession is specific for the molecular state and is only valid inside one time slice. The propagation with Δt at a given state can be performed with the operator P defined as (see Ref. [21]):

$$P(\Delta t) = \exp(iL\Delta t). \tag{9}$$

In this case the propagation is always performed from the beginning (t_{r-1}) of the actual time slice (r).

Using the ψ_p eigenfunctions of the L operator the mathematical form of the propagation operator can be written as:

$$P(\Delta t) = \sum_p |\psi_p\rangle \exp(i\omega_p\Delta t)\langle\psi_p|. \tag{10}$$

The density matrix can be expressed as the linear combination of the φ_e basis set of the Liouville space:

$$|\sigma(t)\rangle = \sum_e |\varphi_e\rangle\langle\varphi_e|\sigma(t)\rangle = \sum_e \sigma_e(t)|\varphi_e\rangle, \tag{11}$$

where the e-th element of the $\sigma(t)$ vector (e.g. $\sigma_e(t)$) is denoted as:

$$\sigma_e(t) = \langle\varphi_e|\sigma(t)\rangle. \tag{12}$$

The density matrix $\sigma(t)$ at time t can be calculated by multiplying the vector in Eq. (11) with the operator in Eq. (10):

$$|\sigma(t)\rangle = P(\Delta t)|\sigma^{(r)}\rangle = \sum_{p,e} |\psi_p\rangle \exp(i\omega_p\Delta t)\langle\psi_p|\varphi_e\rangle\langle\varphi_e|\sigma^{(r)}\rangle. \tag{13}$$

Replacing the scalar products with the coefficients defined in Eq. (8), the f-th element of the $\sigma(t)$ vector ($\sigma_f(t)$) is given according to the Eq. (12) as:

$$\sigma_f(t) = \sum_{p,e} c_{fp}c_{ep} \exp(i\omega_p\Delta t)\sigma_e^{(r)}. \tag{14}$$

3.2. Detection

At time point t the signal given by a molecule can be determined by the scalar product of the density matrix ($\sigma(t)$) and the I^+ operator:

$$fid(t) = \langle I^+|\sigma(t)\rangle. \tag{15}$$

The *fid* points are complex numbers representing the expectation value of the momentary magnetization vector. The density matrix at time point t can be calculated from the one at last exchange ($\sigma^{(r)}$) according to the Eq. (13) and the detected signal at time point t is given as ($\Delta t = t - t_r$):

$$fid(t) = \sum_{p,e} \langle I^+|\psi_p\rangle \exp(i\omega_p\Delta t)\langle\psi_p|\varphi_e\rangle\langle\varphi_e|\sigma^{(r)}\rangle. \tag{16}$$

Replacing the scalar products with the coefficients defined in Eq. (8) yields in:

$$fid(t) = \sum_{p,e} a_p c_{ep} \exp(i\omega_p\Delta t)\sigma_e^{(r)}. \tag{17}$$

where a_p denotes the intensity of the signal given by eigenfunction ψ_p:

$$a_p = \langle I^+|\psi_p\rangle, \tag{18}$$

The density matrix at the beginning of the detection ($t = 0$) is also required for the simulation. In a one-pulse experiment there is only transversal magnetization in the system after the 90° pulse. The density matrix of this state is proportional to the vector of the I^+ operator on the basis of the φ_e basis functions (meaning that $\sigma_e = 1$ if the one-spin transition φ_e is allowed and is 0 otherwise).

The overall *fid* (F) is calculated as the sum of *fid*s of individual scans as:

$$F(t) = \sum_{\text{scans}} \bigcup_r fid(t) = \sum_{\text{scans}} \bigcup_r \sum_{e,p} a_p c_{ep} \exp(i\omega_p\Delta t)\sigma_e^{(r)}, \tag{19}$$

where the symbol $\bigcup$ denotes the union of *fid*s in the time slices [20].

3.3. Exchange

The following criteria are taken into consideration for an exchange reaction (at time point t_r):

- during the exchange the basis functions (φ_e) remain unaltered,
- the exchange takes place in negligible time (instant jump approximation) thus the density matrix also remains unaltered during the exchange.

Due to the exchange the L operator alters and thus the eigenfunctions (ψ_p) and precession frequencies (ω_p) are different before and after it. It means that the density matrix should be calculated at the time point t_{r+1} (using the precession operator of the time slice r) and from that moment the new density matrix should be used for detection (see Eq. (17)) and the next propagation (see Eq. (14)).

To propagate the density matrix to the next exchange point (t_{r+1}) the variable $\Delta t = t - t_r$ should be replaced by $\Delta t_r = t_{r+1} - t_r$ in Eq. (14):

$$\sigma_f^{(r+1)} = \sum_{p,e} c_{fp}c_{ep} \exp(i\omega_p\Delta t_r)\sigma_e^{(r)}. \tag{20}$$

The *fid* in time slice $r+1$ is calculated from this $\sigma^{(r+1)}$ vector (instead of $\sigma^{(r)}$) according to the Eq. (17).

3.4. Propagation in Hilbert space

In the previous paragraph the mathematical background of the propagation was shown in the Liouville space which means that the size of the precession operator is approximately 2^{4n}. It can also be solved in the Hilbert space as well since the Hamiltonian of the system is real and time-independent inside the time slices.

In the previous section the Liouville–von Neumann equation (Eq. (1)) was solved by transforming the commutator into the Liouville space (as L operator) and solving the resulting linear differential equation. Instead of that the following solution of Eq. (1) will be used now (see Ref. [22]):

$$\hat{\rho}(t) = \exp(-i\hat{H}t)\hat{\rho}(0)\exp(i\hat{H}t). \tag{21}$$

This solution is only valid when the Hamiltonian is constant between time points 0 and t [5]. In this case exchange is handled separately (by Monte Carlo method) and therefore the Hamiltonian does not change inside time slices. This means that the precession can be simulated using the operation given in Eq. (21).

The exponential of the Hamiltonian is diagonal on the basis of the eigenfunctions of the same Hamiltonian (Ψ_l, with eigenvalue λ_l) which means that:

$$\exp(\pm i\hat{H}t) = \sum_l |\Psi_l\rangle \exp(\pm i\lambda_l t)\langle\Psi_l|. \tag{22}$$

The Ψ_k eigenfunctions of the Hamiltonian can be expressed as linear combinations of the common product basis functions ($\alpha\ldots\alpha\alpha$, $\alpha\ldots\alpha\beta$, …, $\beta\ldots\beta\beta$, noted Φ_a where $a = 1\ldots 2^n$ and n is the number of spins in the non-exchanging system):

$$\Psi_k = u_{ak}\Phi_a \text{ where } u_{ak} = \langle\Phi_a|\Psi_k\rangle \tag{23}$$

The matrix of the u_{ak} coefficients (U) is real and unitary. Substituting Eq. (22) into Eq. (21) and taking the matrix form of the operators gives:

$$\rho(t) = U\exp(-i\Lambda\Delta t)U^T\rho^{(r)}U\exp(i\Lambda\Delta t)U^T, \tag{24}$$

where Λ denotes the diagonal matrix of the λ_k eigenvalues of H and U^T is the transpose of the real unitary matrix U. Eq. (24) shows the calculation of the matrix $\rho(t)$ knowing $\rho^{(r)}$ ($\Delta t = t - t_r$, meaning the time elapsed since the last exchange).

Replacing the matrix multiplication with the corresponding coefficients in Eq. (24) and rearranging terms give the following equation for the density matrix (using the notation ρ_{ab} for the matrix elements of ρ):

$$\rho_{ab}(t) = \sum_{c,d,k,l} u_{ak}u_{bl}\cdot u_{ck}u_{dl}\cdot\exp(i(\lambda_l-\lambda_k)\Delta t)\rho_{cd}^{(r)}. \tag{25}$$

Eqs. (25) and (14) give the same result, which can be proven if we substitute the p, f and e (as hyperindices) with (k,l), (a,b) and (c,d), respectively and knowing that $c_{fp} = u_{ak}u_{bl}$, $c_{ep} = u_{ck}u_{dl}$ and $\omega_p = \lambda_l - \lambda_k$.

The expression for detection can be derived from Eq. (24):

$$\begin{aligned} fid(t) &= Tr(\rho(t)\hat{I}^+) \\ &= Tr(U\exp(-i\Lambda\Delta t)U^T\rho^{(r)}U\exp(i\Lambda\Delta t)U^T\hat{I}^+). \end{aligned} \tag{26}$$

Rearranging this expression gives:

$$fid(t) = Tr((U^T\hat{I}^+U)\exp(-i\Lambda\Delta t)U^T\rho^{(r)}U\exp(i\Lambda\Delta t)), \tag{27}$$

and denoting the expression between the first inner parentheses in Eq. (27) with A gives:

$$fid(t) = Tr(A\ \exp(-i\Lambda\Delta t)U^T\rho^{(r)}U\exp(i\Lambda\Delta t)). \tag{28}$$

The physical meaning of the (k,l) element of the A matrix (a_{kl}) is the intensity of the $\Psi_l \rightarrow \Psi_k$ transition. Replacing the matrices with their elements in Eq. (28) gives:

$$fid(t) = \sum_{c,d,k,l} a_{kl}u_{ck}u_{dl}\exp(-i(\lambda_l-\lambda_k)\Delta t)\rho_{cd}^{(r)}, \tag{29}$$

which is the Hilbert space equivalent of Eq. (17), the formula of detection in Liouville space. The overall *fid* (F) is calculated as the sum of *fid*s of individual scans as:

$$\begin{aligned} F(t) &= \sum_{\text{scans}}\bigcup_r fid(t) \\ &= \sum_{\text{scans}}\bigcup_r\sum_{c,d,k,l} a_{kl}u_{ck}u_{dl}\exp(i(\lambda_l-\lambda_k)\Delta t)\rho_{cd}^{(r)}, \end{aligned} \tag{30}$$

where the symbol $\bigcup$ denotes the union of *fid*s in the time slices [20].

It is well-known that the Hamiltonian blocks according to the total spin quantum numbers (to be called levels) which means that each eigenvector belongs to the subspace spanned by basis vectors of the same level. Neither the precession nor the exchange can combine functions of different levels therefore the blocks of the density matrix can be handled separately and only the $\Delta I = 1$ blocks have to be calculated. This reduces the RAM requirement of the calculation to $\binom{n}{n/2}^2$, the size of the simulations in the Hilbert space.

4. Comparison of the propagator based and the extended vector models

The formula for the precession was the following (using the notations defined here) in our previous, extended vector model based MC-DNMR program (see Eq. (23) in Ref [20]):

$$\sigma_e^{(r+1)} = \sum_p c_{ep}^2\exp(i\omega_p\Delta t_r)\sigma_e^{(r)} \tag{31}$$

Comparing Eqs. (31) and (14) shows that only the diagonal part of the exact precession operator is taken into account in the extended vector model (further on XVM) introduced there. According to the XVM the probability of frequency ω_p for basis transition φ_e is c_{ep}^2 at any time. XVM also assumes that the basis state (φ_e) is conserved during precession thus the frequency distribution is valid on a whole time interval. On the other side, in the new model based on the propagator formalism (further on PM) the propagators evaluate the basis functions according to the Hamiltonian as probabilities but the frequencies are only used as technical values to perform calculations. If we try to explain the PM based Eq. (14) in the XVM we get that the probability of frequency ω_p for basis transition φ_e is c_{ep}^2 at any time as well, but the basis transition is not preserved in time intervals of precession.

In PM the magnetization (or the vector) on φ_e at t_r ($\sigma_e^{(r)}$) can end in any basis state at t_{r+1}. The transition from φ_e to φ_f is done through eigenstates and its probability is given by the coefficients $c_{ep}^2c_{fp}^2$. This transition is explained on Fig. 2. At a given point of time a state in the vector model can be handled based on its basis state or on its eigenstate. These two states exist independently all the time (only their distribution is defined). During exchange the basis state, while during precession the eigenstate is preserved. Therefore the precession and exchange operators have effects on the different representations. XVM handles this duality with probabilities as well as PM. Both models calculate the probability of a molecule being in an eigen or in a basis state (equals to the square of the corresponding density matrix element) and the two probabilities are connected through the c_{ep} linear combination coefficients (dots on the arrows on Fig. 2 or the scalar product $\langle\psi_p\varphi_e\rangle$ in Eq. (13)).

Using the XVM model Eq. (13) describes the following process (from the exchange at time t_{r-1}): the exchange operator gives the density matrix in the product basis form at time t_{r-1} (Fig. 2 segment X_{r-1}). To perform precession the density matrix has to be converted to the eigenfunction representation (Fig. 2 segment P_{r-1}) and in this form the detected *fid* points and the density matrix can easily be calculated at t_r. For the exchange 'operator' the density matrix should be converted back to basis function representation (segment X_r) and the same process starts from the beginning (segments P_r and X_{r+1}). The most important difference between the two models is that in XVM the system still 'remembers' its basis state at t_r before the exchange at t_{r+1} (e.g. gray dots

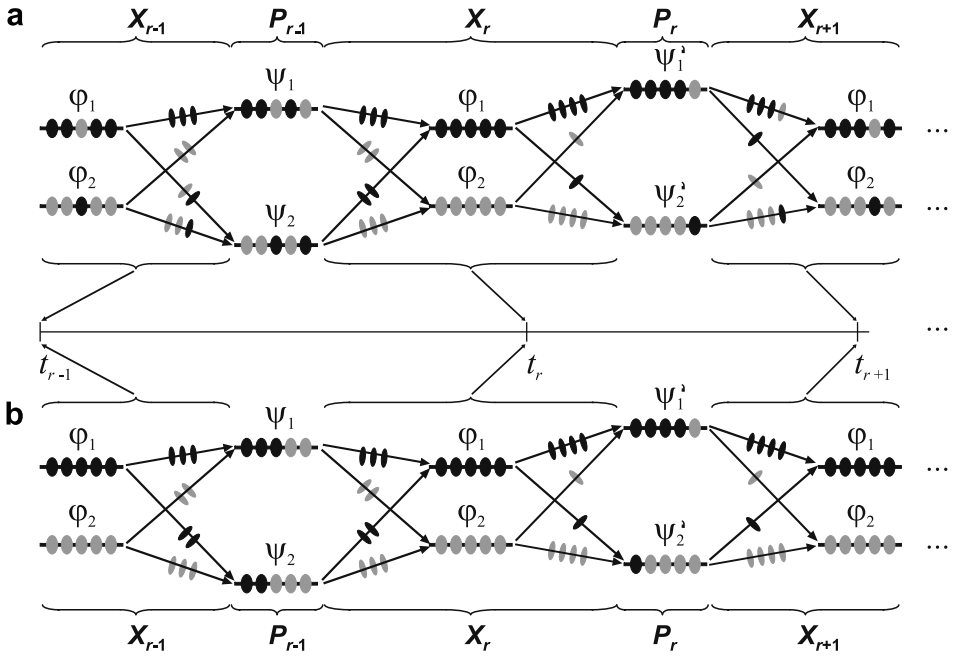

Fig. 2. Comparison of the transition models (a) PM and (b) XVM. In both models the population of basis states (see spots on lines) is transferred to eigenstates (and vice versa) based on the linear combination coefficients (spots on arrows). The difference between the two models is that while in the case of the XVM model the magnetization of φ_1 transition at t_{r-1} returns to φ_1 at t_r through ψ_1 (and through ψ_2 as well), in the case of the PM model basis functions can alter during precession.

always belong to φ_2 coherence on Fig. 2b) while in PM the basis state is not preserved. Correcting Eq. (31) with the neglection of the preservation of basis state gives the formula of Eq. (14).

Usually the two methods yield similar spectra except in systems where *J*-coupling occurs between the exchanging sites. In this case the high temperature spectrum simulated by the program based on the XVM (MC-DNMR) is wrong but the one calculated by ProMoCS (using PM model) is correct. The explanation of this phenomenon is shown on an example of mutually exchanging *AB* spin system.

4.1. Simulation of mutually exchanging coupled AB spin system

At the beginning the 'static' transitions of the exchanging sites have to be determined. This is obvious in cases when there is no coupling between the exchanging sites. However, for an *AB* spin system the exchanging nuclei (*A* and *B*) are coupled to each other, therefore their transitions depend on each other. Instead of separating the two nuclei, the $AB \leftrightarrow BA$ mutual exchange is simulated as a special case of $AB \leftrightarrow CD$ exchange where $C = B$ and $D = A$.

As it was stated before, the MC-DNMR program gives wrong results for high temperature spectra of mutually exchanging *AB* spin systems [20]. The error can be analyzed by determining the behavior of each basis coherence in the simulation. Fast exchange averages the two energy levels with $I_{z,tot} = 0$ (Φ_2 and Φ_3 on Fig. 3). This does not mean that the two energy levels are converted into each other by the exchanges. The basis states (Φ_2 and Φ_3) are the ones converted into each other and thus the basis coherences φ_1 and φ_2 are exchanging (and never remaining the same, see Fig. 2), φ_3 and φ_4 do the same, but independently from the other two. The exchange is mutual therefore the probabilities (or coefficients) are symmetrical and thus the common frequency is the average of the possible frequencies. This means that ν_1 and ν'_1 are averaged (as the basis coherences φ_1 and φ_2 are replacing each other) and ν_2 and ν'_2 are averaged as well (by the exchange of φ_3 and φ_4). The average of the first two frequencies ($\frac{\nu_1+\nu'_1}{2}$) is higher than that of the two latter ($\frac{\nu_2+\nu'_2}{2}$). This results in a doublet instead of a singlet for the high temperature spectrum (Fig. 4).

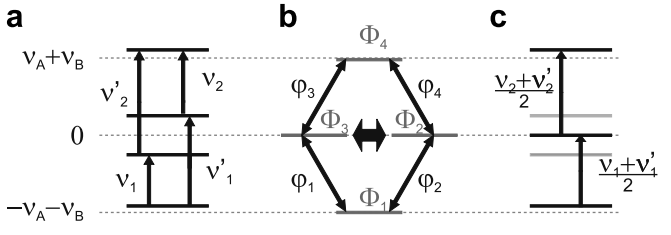

Fig. 3. Explanation of the spectrum simulated by MC-DNMR for a mutually exchanging AB spin system. (a) Energy levels and frequencies (ν_p) of the *AB* spin system at slow exchange. (b) Basis functions (Φ_k) and coherences (φ_e) showing the exchange process. (c) Similar to (a) but for fast exchange (the energy levels of slow exchange are shown in gray as reference).

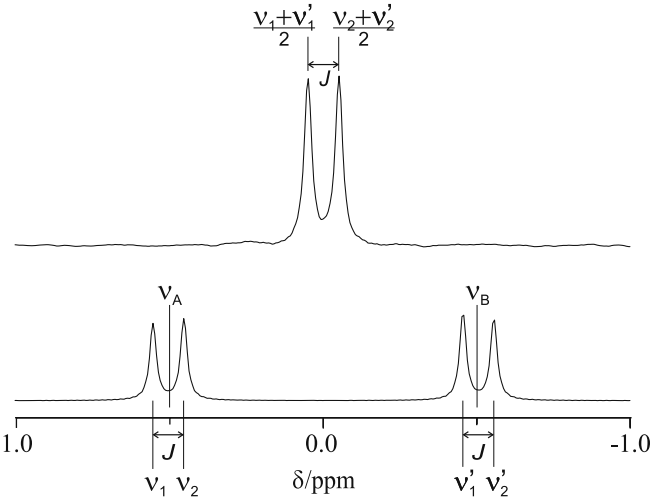

Fig. 4. Low and high temperature spectra simulated by MC-DNMR for a mutually exchanging *AB* spin system.

The PM based ProMoCS program does not separate the basis transitions of the same level and it gives correct results for the high temperature spectrum as well. The signal detected at a given time can be calculated as a function of exchange times and the Hamiltonians of *AB* and *BA* conformer as:

$$fid(t) = \langle I^+ | e^{iL_1(t-t_r)} e^{iL_2\Delta t_{r-1}} \cdot \ldots \cdot e^{iL_1\Delta t_1} | \sigma(0) \rangle, \tag{32}$$

where L_1 and L_2 are the Hamiltonians for *AB* and *BA* conformer (in the Liouville space), Δt_i is the length of the i-th time slice ($\Delta t_i = t_{i+1} - t_i$), t is the time point of detection which is inside time slice r (meaning $t_r < t < t_{r+1}$). In Eq. (32) L_1 and L_2 are matrices therefore $e^{iL_1\Delta t_1} e^{iL_2\Delta t_2} \neq e^{iL_1\Delta t_1 + iL_2\Delta t_2}$, but the difference is of order τ^2 which is negligible in the case of small Δt_i [5]. For fast reactions Δt_i values are small (for any value of i) and therefore Eq. (32) can be approximated as:

$$fid(t) = \langle I^+ | e^{iL_1(t-t_r) + iL_2\Delta t_{r-1} + \ldots + iL_1\Delta t_1} | \sigma(0) \rangle. \tag{33}$$

This approximation is valid even for finite exchange rates. The exchange in question is mutual therefore the time spent in conformer *AB* equals to the time spent in *BA* and thus the sum in Eq. (33) can be written in a shorter form:

$$fid(t) = \langle I^+ | \exp\left(i \frac{L_1 + L_2}{2} t \right) | \sigma(0) \rangle. \tag{34}$$

The Hamiltonian of the *AB* conformer in the Liouville space is (with frequencies ν_A, ν_B and coupling constant J):

$$L_1 = \begin{pmatrix} \nu_A \pm \frac{J}{2} & \frac{\mp J}{2} \\ \frac{\mp J}{2} & \nu_B \pm \frac{J}{2} \end{pmatrix}, \tag{35}$$

where the ± sign belongs to the total spin quantum number change $0 \to 1$ and $-1 \to 0$. The L_2 operator of the *BA* conformer is similar just the role of *A* and *B* has to be swapped:

$$L_2 = \begin{pmatrix} \nu_B \pm \frac{J}{2} & \frac{\mp J}{2} \\ \frac{\mp J}{2} & \nu_A \pm \frac{J}{2} \end{pmatrix}. \tag{36}$$

The average of the two operators needed in Eq. (34) is:

$$\frac{L_1 + L_2}{2} = \begin{pmatrix} \frac{\nu_A + \nu_B}{2} \pm \frac{J}{2} & \frac{\mp J}{2} \\ \frac{\mp J}{2} & \frac{\nu_A + \nu_B}{2} \pm \frac{J}{2} \end{pmatrix}. \tag{37}$$

This operator is the same as the Hamiltonian of a common A_2 spin system (where the frequency is $\frac{\nu_A+\nu_B}{2}$ and the coupling constant is J) with eigenvalues $\frac{\nu_A+\nu_B}{2}$ and $\frac{\nu_A+\nu_B}{2} \pm J$ the latter of which has zero intensity. This results in a singlet in the high temperature spectrum as expected. Fig. 5 shows the simulated spectra of a general AB spin system simulated by ProMoCS and the average Hamiltonian based MEXICO programs (the latter is handled as reference). The two series of spectra fit well to each other.

5. Examples

The program was tested on several molecules. Here the examples of *N*,*N*-dimethyl-para-nitroso-aniline and trimethylsilylcyclopenta-[*l*]-phenantrene (Me_3Si^cPPh) are shown. The spectra simulated by ProMoCS will be compared with the ones simulated by MEXICO using the same parameter set [21,23].

5.1. Coupled mutual exchange

The dynamic structure of *N*,*N*-dimethyl-para-nitroso-aniline is shown on Fig. 6. The conformational exchange detailed here is the syn-anti isomerism of the nitroso group. This reaction was studied earlier and the kinetic and spectral parameters were fitted to the experimental spectra [21]. The simulation to be shown here is compared to the spectra simulated by the MEXICO. The parameters used for the simulations are shown in Table 1 (as given in Ref. [21]).

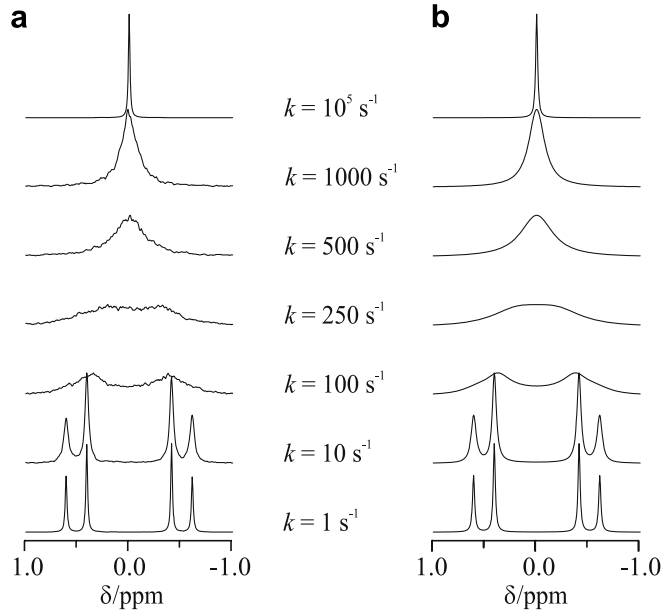

Fig. 5. Temperature dependent spectra of a mutually exchanging AB spin system calculated by (a) ProMoCS and (b) MEXICO. The parameters used for the simulation: $\nu_A = 0.5$ ppm (50 Hz), $\nu_B = -0.5$ ppm (−50 Hz), $J = 10$ Hz, SI = 512. NS = 1000 for ProMoCS.

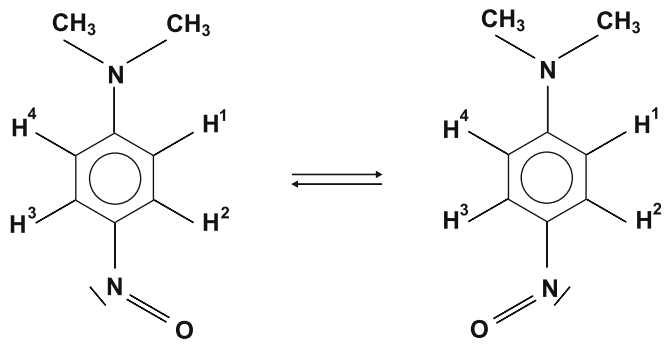

Fig. 6. Structure of *N*,*N*-dimethyl-para-nitroso-aniline and numbering of simulated protons.

The aromatic part of the spectra can be simulated taking into account the four aromatic protons only as these are not coupled to the methyl hydrogens. These four nuclei are scalar coupled to each other and they are connected by the rotation around the C–N(O) bound as well.

Spectra were simulated with SI = 512 points and NS = 1000 scans (the latter in ProMoCS). The middle of the spectra is at 7.5 ppm, spectrum width is 3 ppm. The ^{1}H resonance frequency was supposed to be 300 MHz. The simulated spectra fit well to the reference ones as it is shown on Fig. 7.

Table 1
Spectral parameters used for the simulation of the temperature dependent ^{1}H NMR spectra of *N*,*N*-dimethyl-para-nitroso-aniline.

δ/ppm	J/Hz
$\delta_1 = 6.76$	$J_{1,2} = 9.1$
$\delta_2 = 8.79$	$J_{2,3} = 2.1$
$\delta_3 = 6.63$	$J_{3,4} = 9.5$
$\delta_4 = 6.47$	$J_{1,4} = 2.5$

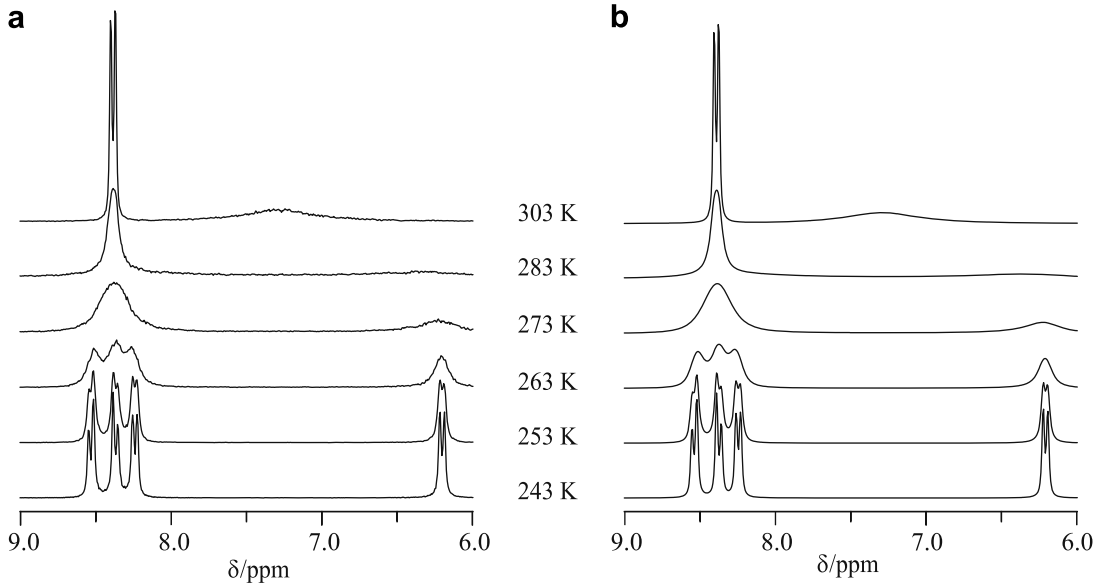

Fig. 7. Simulated temperature dependent ^{1}H NMR spectra of *N*,*N*-dimethyl-para-nitroso-aniline calculated by (a) ProMoCS and (b) MEXICO (1000 scans, SI = 512, LB = 2.0 Hz). Simulations with ProMoCS were performed on a desktop PC with Intel Core-2 Duo 2.20 GHz processor and Windows XP operating system using two Java threads. Runtime for all six temperatures was 48.6 s.

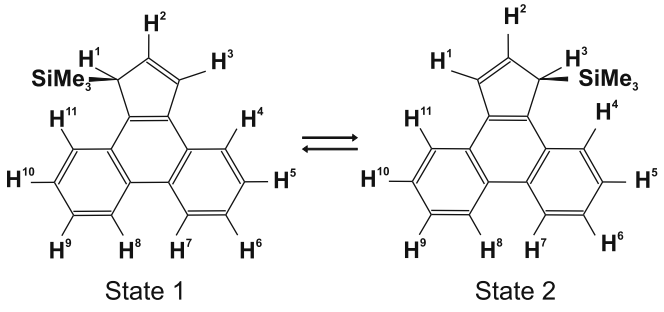

Fig. 8. Structure and numbering of hydrogens $Me_3{}^cPPh$.

5.2. A larger spin system

The chemical formula of $Me_3{}^cPPh$ is shown on Fig. 8. The process in question is the migration of the Me_3Si group from C^1 to C^3. This mutual exchange reaction was studied earlier by dynamic NMR and EXSY measurements [23] and the measured thermodynamic data were $\Delta H^{++} = 63.6$ kJ mol^{-1} and $\Delta S^{++} = 34.3$ J K^{-1} mol^{-1}.

Here the spectra of the eight spin system H^4 to H^{11} were simulated at five different temperatures (Fig. 9). Spectroscopic parameters used for the simulation are shown in Table 2. The spin set H^4 to H^7 is not coupled to other protons therefore the system can be simulated as four spins in two states: where the Me_3Si is at position 1 (State 1) and at 3 (State 2) on Fig. 8. The spectra simulated fits well to the reference in all cases again (Fig. 9).

6. Conclusions

The ProMoCS program presented here incorporates the Monte Carlo simulation and the propagation of the time dependent density matrix. The two main processes of the spin system are handled separately: the precession is simulated by means of the propagator formalism while the exchange reaction rates are taken into account statistically. The PM model for the explanation of the calculation

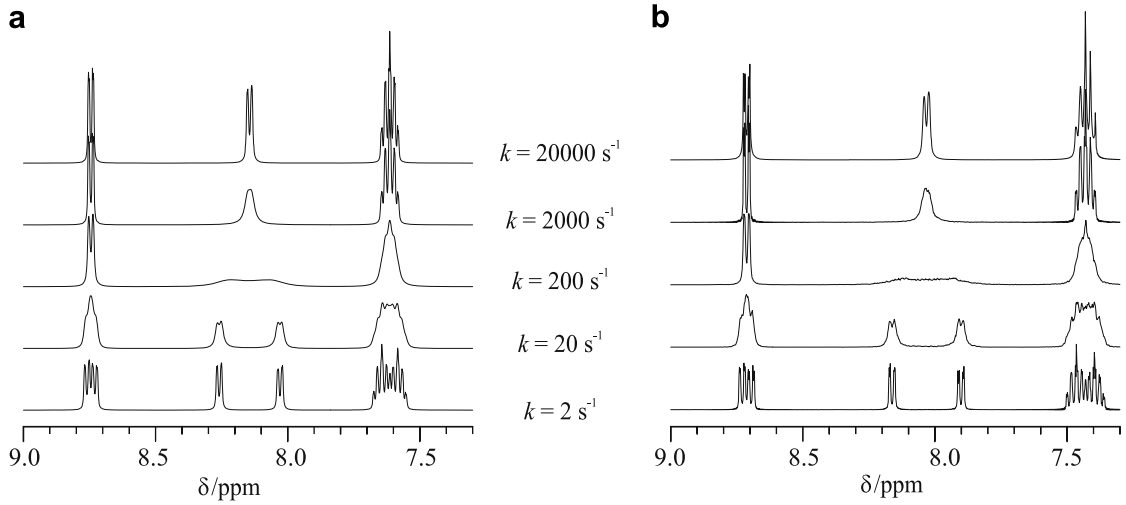

Fig. 9. Simulated temperature dependent spectra of $Me_3{}^cPPh$ (a) MEXICO and (b) ProMoCS. Simulations with ProMoCS (1000 scans, SI = 512, LB = 2.0 Hz) were performed on a desktop PC with Intel Core-2 Duo 2.20 GHz processor and Windows XP operating system using two Java threads. Runtime for all five temperatures was 54.9 s.

Table 2
Chemical shift values (δ) and coupling constants (J) used for the simulation of DNMR spectra of Me_3Si^cPPh [23].

	State 1	State 2
δ_4/ppm	8.26	8.03
δ_5/ppm	7.66	7.60
δ_6/ppm	7.63	7.57
δ_7/ppm	8.76	8.73
$J_{4,5}$/Hz	8.3	8.3
$J_{4,6}$/Hz	1.5	1.8
$J_{4,7}$/Hz	0.5	0.6
$J_{5,6}$/Hz	6.8	6.7
$J_{5,7}$/Hz	1.5	1.8
$J_{6,7}$/Hz	8.3	8.3

method is also shown indicating the connection with the previously introduced extension of the vector model to spin systems with chemical exchange. The program based on this theory was successfully tested for several molecules including a mutually exchanging AB spin system.

Acknowledgment

We thank Dr E. Rohonczy-Boksay for her useful comments.

References

[1] J.I. Kaplan, G. Fraenkel, NMR of Chemically Exchanging Systems, Academic Press, New York, 1980.
[2] J.K.M. Sanders, B.K. Hunter, Modern NMR Spectroscopy, Oxford Univ. Press, Oxford, 1993.
[3] A.E. Derome, Modern NMR Techniques for Chemistry Research, Pergamon Press, Oxford, 1993.
[4] J. Sandstrom, Dynamic NMR Spectroscopy, Academic Press, London, 1982.
[5] R.R. Ernst, G. Bodenhausen, A. Wokaun, Principles of Nuclear Magnetic Resonance in One and Two Dimensions, Clarendon Press, Oxford, 1987.
[6] L.M. Jackman, F.A. Cotton, Dynamic Nuclear Magnetic Resonance Spectroscopy, Academic Press, New York, 1975.
[7] J.W. Emsley, J. Feeney, L.H. Sutcliffe, High Resolution NMR Spectroscopy, Pergamon Press, New York, 1965.
[8] S. Szymanski, G. Binsch, A Liouville space formulation of Wangsness–Bloch–Redfield theory of nuclear spin relaxation. II. Scalar relaxation, J. Magn. Reson. 81 (1989) 104–120.
[9] D.S. Stephenson, G. Binsch, Iterative computer analysis of complex exchange-broadened NMR bandshapes, J. Magn. Reson. 32 (1978) 145–152.
[10] D.A. Kleier, G. Binsch, General theory of exchange-broadened NMR line shapes II. Exploitation of invariance properties, J. Magn. Reson. 3 (1970) 146–160.
[11] G. Binsch, A unified theory of exchange effects on nuclear magnetic resonance line shapes, J. Am. Chem. Soc. 91 (1969) 1304–1309.
[12] A.D. Bain, D.M. Rex, R.N. Smith, Fitting dynamic NMR lineshapes, Magn. Reson. Chem. 39 (2001) 122–126.
[13] A.D. Bain, G.J. Duns, A unified approach to dynamic NMR based on a physical interpretation of the transition probability, Can. J. Chem. 74 (1996) 819–824.
[14] A.D. Bain, G.J. Duns, A new approach to the calculation of NMR lineshapes of exchanging systems, J. Magn. Reson. A 112 (1995) 258–260.
[15] H.J. Reich, W.S. Goldenberg, B.Ö. Gudmundsson, A.W. Sanders, K.J. Kulicke, S. Simon, I.A. Guzei, Amine-chelated aryllithium reagents–structure and dynamics, J. Am. Chem. Soc. 123 (2001) 8067–8079.
[16] H.J. Reich, J. Chem. Educ. Software 3D2 (1996).
[17] Available from: <http://www.bruker-biospin.com/topspin_structure_analysis.html>.
[18] R.S. Dumont, P. Hazendouk, A.D. Bain, Dual Lanczos simulation of dynamic nuclear magnetic resonance spectra for systems with many spins or exchange sites, J. Chem. Phys. 113 (2000) 3270–3281.
[19] R.S. Dumont, S. Jain, A.D. Bain, Simulation of many-spin system dynamics via sparse matrix methodology, J. Chem. Phys. 106 (1997) 5928–5936.
[20] Zs. Szalay, J. Rohonczy, Monte Carlo simulation of DNMR spectra of coupled spin systems, J. Magn. Res. 191 (2008) 56–65.
[21] A.D. Bain, Chemical exchange in NMR, Progr. Nucl. Magn. Res. 43 (2003) 63–103.
[22] M. Mehring, High Resolution NMR in Solids, Springer-Verlag, Berlin, 1983.
[23] S.S. Rigby, H.K. Gupta, N.H. Werstiuk, A.D. Bain, M.J. McGlinchey, Do Aromatic transition states lower barriers to silantropic shifts? A synthetic, NMR spectroscopic, and computational study, Inorg. Chim. Acta 251 (1996) 355–364.